FEBS Letters 588 (2014) 1465–1469

journal homepage: www.FEBSLetters.org

The role of connexin40 in developing atrial conduction

Jiri Benes Jr. [a,b,d,*], Grazia Ammirabile [c], Barbora Sankova [a,b], Marina Campione [c], Eliska Krejci [a,b], Alena Kvasilova [b], David Sedmera [a,b]

[a] Department of Cardiovascular Morphogenesis, Institute of Physiology, Academy of Sciences of the Czech Republic, Prague, Czech Republic
[b] Charles University in Prague, First Faculty of Medicine, Institute of Anatomy, U Nemocnice 3, Prague, Czech Republic
[c] CNR Institute of Neurosciences, Department of Biomedical Sciences, University of Padova, Viale G. Colombo 3, Padova 35121, Italy
[d] Charles University in Prague, First Faculty of Medicine, Department of Radiology of the First Faculty of Medicine and General Teaching Hospital, U Nemocnice 2, Prague, Czech Republic

ARTICLE INFO

Article history:
Received 1 December 2013
Revised 22 January 2014
Accepted 22 January 2014
Available online 31 January 2014

Edited by Michael Koval, Brant E. Isakson, Robert G. Gourdie and Wilhelm Just

Keywords:
Heart development
Arrhythmogenesis
Sinoatrial node
Optical mapping
Mouse embryo

ABSTRACT

Connexin40 (Cx40) is the main connexin expressed in the murine atria and ventricular conduction system. We assess here the developmental role of Cx40 in atrial conduction of the mouse. Cx40 deficiency significantly prolonged activation times in embryonic day 10.5, 12.5 and 14.5 atria during spontaneous activation; the severity decreased with increasing age. In a majority of Cx40 deficient mice the impulse originated from an ectopic focus in the right atrial appendage; in such a case the activation time was even longer due to prolonged activation. Cx40 has thus an important physiological role in the developing atria.

1. Introduction

Intercellular connections in the heart via gap junctions play an important role in impulse propagation in the myocardium. Cardiac gap junctions are composed of proteins called connexins (Cxs) that form low resistance channels, which enable electrical coupling of adjacent myocytes allowing intercellular electrical communication. Many studies have shown that alterations in the localization and expression of connexin proteins in the heart may cause abnormal activation spreading through the myocardium, thus leading to arrhythmias [1–3].

In mammalian hearts, mRNA for connexins 30.2, 40, 43 and 45 has been detected [4]. The expression of these connexins is dynamic in different parts of the heart, and the expression pattern is well conserved among species [5]. Each connexin forms a channel with unique electrophysiological properties [6]. The main connexin in murine atria is Cx40, but Cx43 and Cx45 are also expressed in smaller amounts [7]. Nevertheless, as a differentiation marker of the chamber myocardium [8], Cx40 is absent in the sinoatrial node.

The role of Cx40 in human arrhythmias was studied extensively [9,10]. The most common supraventricular arrhythmia in humans is atrial fibrillation. The studies investigating the relation between this arrhythmia and Cx40 have yielded rather conflicting results [11]. Simon et al. studied cardiac conduction abnormalities in mice lacking Cx40 and found no case of atrial fibrillation [3]. Verheule et al. described predisposition to tachyarrhythmias in adult Cx40 deficient mice after atrial burst pacing [12]. Recent studies in humans have discovered a polymorphism in the *Cx40* gene that is connected with a higher risk of developing atrial fibrillation [13]. Recently, Yang et al. [14] described a null mutation of Cx40 significantly associated with atrial fibrillation onset in humans.

Despite this fact, most of the studies performed in Cx40 deficient mice were focused on the ventricular conduction system, where several conduction pathologies such as right bundle branch block or slowed atrioventricular conduction were described [12,15]. In the adult mouse atria, prolongation of P wave and ectopic foci were reported [16]. Probably the most comprehensive study of the role of Cx40 deficiency on the developing atria was made by Greg Morley's group [17]. These authors described conduction velocity heterogeneity of the paced beat between the left and right atria in adult mice, which is lost in Cx40 deficiency. At the prenatal stages – embryonic day (ED)13.5 and ED15.5 – they found impaired SAN impulse initiation with ectopic sites of

* Corresponding author at: Institute of Anatomy, U Nemocnice 3, 12800 Prague 2, Czech Republic. Fax: +420 2 2496 5770.
E-mail address: jiri.benes2@lf1.cuni.cz (J. Benes Jr.).

http://dx.doi.org/10.1016/j.febslet.2014.01.032
0014-5793/

activation. The main objective of our study was to assess the role of Cx40 in impulse generation and spontaneous propagation in murine atria during early embryonic development.

2. Methods

2.1. Animals

Cx40:GFP knock-in mice developed by Lucile Miquerol [18] were used. As the knock-in of the *GFP* disrupts the endogenous *Cx40* gene, the homozygotes are functional nulls. *Cx40* null mice were maintained in homozygous state, as these animals are viable and fertile (albeit with a reduced life span, a smaller number of embryos per litter and a non-Mendelian ratio of nulls in heterozygous matings). Heterozygous embryos were obtained from timed matings of a Cx40-deficient male and a wild type (WT) female; for WT, mixed genetic background related to the Swiss strain and *Cx40:GFP* mice was used [19]. The experimental protocol was approved by the local animal committee and conforms to the Guiding Principles in the Care and Use of Vertebrate Animals in Research and Training.

2.2. Optical mapping of embryonic hearts

The animals were caged together overnight, and the noon of the day of vaginal plug detection was considered ED0.5. Pregnant females were killed by cervical dislocation on ED10.5, 12.5 and 14.5 and the embryos were rapidly dissected in ice-cold (to prevent ischemic damage to the heart) Tyrodes solution (composition: NaCl 145 mmol/l, KCl 5.9 mmol/l, $CaCl_2$ 1.1 mmol/l, $MgCl_2$ 1.2 mmol/l, glucose 11 mmol/l, HEPES 5 mmol/l; pH = 7.4). These stages were selected to cover the early period of cardiac development prior to septation. The hearts with adjacent posterior body wall structures were isolated and stained in 2.5 mmol/l di-4-ANEPPS (Invitrogen) for 10 min. Motion control was achieved by addition of 0.1 μM blebbistatin (Sigma) and pinning the torso to the bottom of the dish. Because of different focal planes for atria and ventricles (Fig. 1), our standard imaging protocol had to be modified slightly as we were unable to use the recordings performed for the analysis of ventricular activation patterns in a separate study [19]. To avoid any perturbation of the pacemaking region, we chose the antero-superior view (Figs. 1 and 2). Despite the overall transparency of the heart, the outflow region obscured the central area, where the pacemaker is normally located; for this reason, we removed the outflow tract at the ventricular border and at its distal connection to pharyngeal arch arteries. Data acquisition and analysis were performed using the Ultima L high-speed camera and bundled software as described recently [20]. To better appreciate the dynamics of atrial activation, the percentile activation over time method, recently validated by the Gourdie lab [21], was used (Fig. 2). The area of each color band was measured and expressed as a percentage of the whole atrial area. We then interpolated the data in the resulting graph to obtain times, at which 20%, 40%, 60%, 80%, and 100% of the atria was activated. Times across these intervals were then averaged among groups. Differences in quantitative parameters among groups were analyzed by ANOVA and Scheffe' test for multiple comparisons. Values between left and right atrium were compared using paired two-tailed Student's *t*-test. In all cases, values of $P < 0.05$ were considered statistically significant.

2.3. Immunohistochemistry

To obtain a morphological view of the atrial myocardium and SAN position, six WT embryos and ten embryos of the *Cx40*−/− line at ED12.5 were fixed in 4% paraformaldehyde in PBS overnight at 4 °C, and transferred into OCT medium through ascending saccharose gradients. Ten-micron sections were cut on a cryomicrotome,

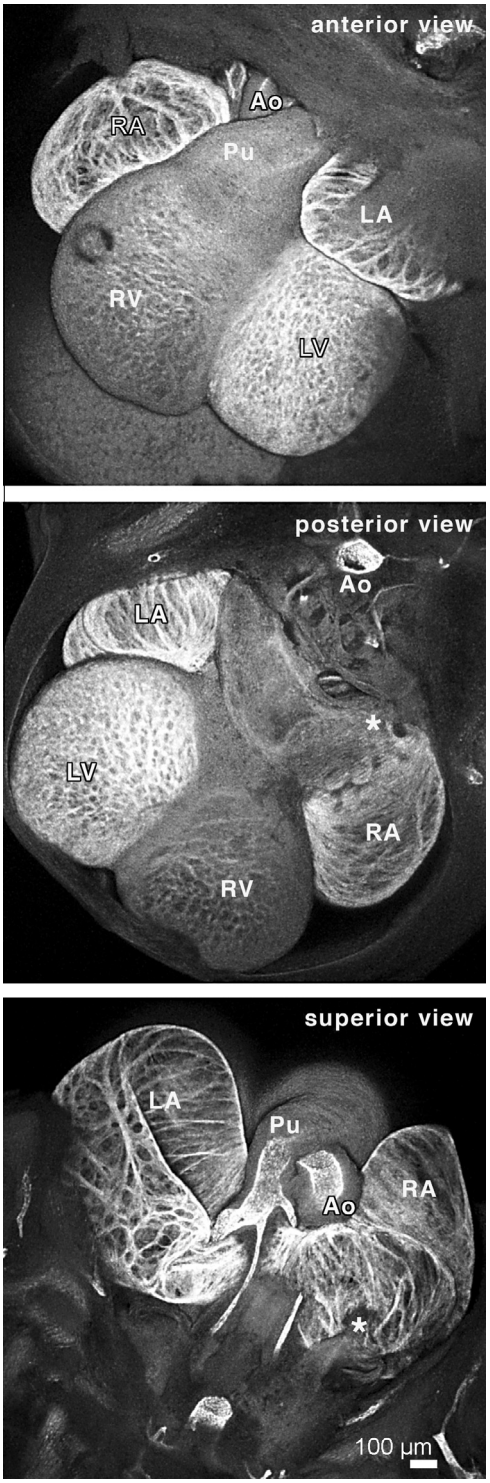

Fig. 1. Morphology of an ED12.5 mouse heart. The heart of a *Cx40*+/− mouse embryo at ED12.5 in confocal projections (GFP fluorescence) in three complementary views. In the anterior view, it is evident how the outflow tract covers the central portion of the atria. In the posterior view, the same area is hidden by the veins entering the right atrium. In the superior view the extensive antero-posterior dimension of the atria is clearly visible, and a fine network of pectinate muscles in both atria can be appreciated. RA – right atrium; LA – left atrium; RV – right ventricle; LV – left ventricle; Ao – aorta; Pu – pulmonary trunk; asterisks mark the putative site of the SAN, distinguished from the surrounding GFP-positive atrial myocardium by its darkness.

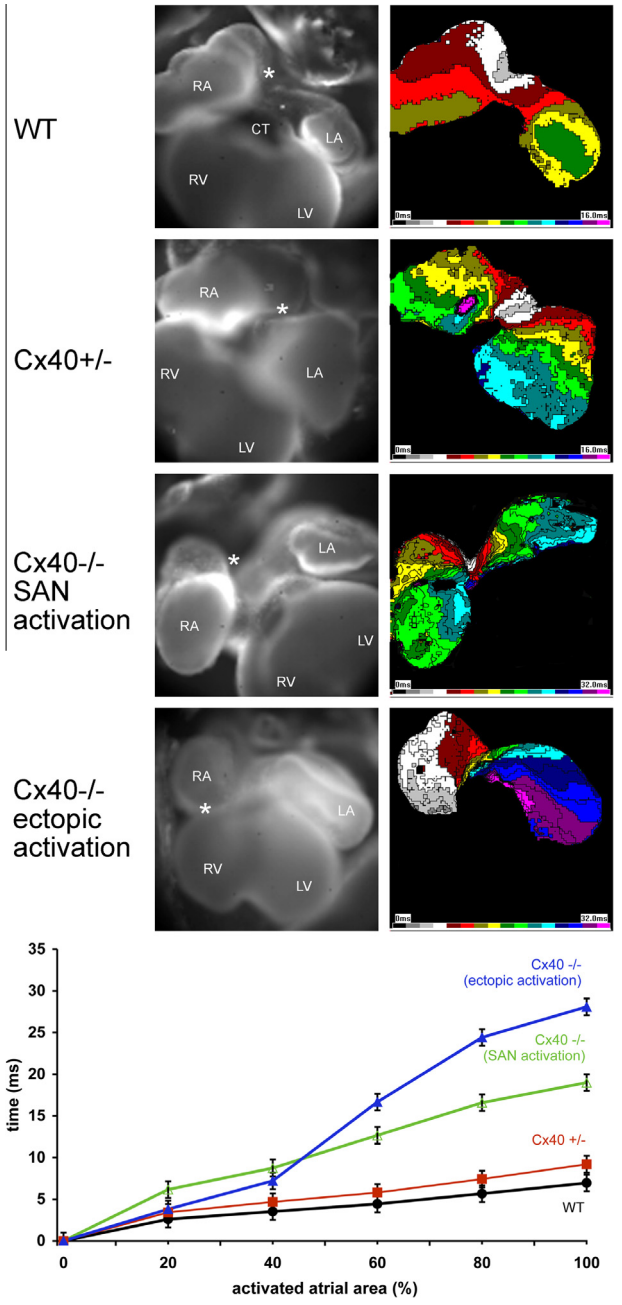

Fig. 2. Activation patterns of the atria at ED12.5 in WT, *Cx40*+/− and *Cx40*−/− hearts. In *Cx40*−/− hearts there are two main patterns of activation – normal SAN activation (third row) and ectopic activation (fourth row). In the first column are shown microscopical images of hearts with removed outflow tract (conotruncus – CT – labeled in the first image). In the second column are the corresponding activation maps. LA – left atrium; LV – left ventricle; RA – right atrium; RV – right ventricle; asterisk – site of first breakthrough (activation site). The chart below shows quantification of atrial activation times and dynamics. The time course of atrial activation demonstrates a significant delay between the left and right atrium in the right atrial ectopic activation.

and alternating sections were mounted on poly-lysine coated slides and alternatively stained with hematoxylin-eosin, anti-HCN4 (1:500, Alomone labs), and anti-Cx43/wheat germ agglutinin/Hoechst (Sigma/Invitrogen). The specific antibody binding was visualized with goat-anti-rabbit antibody (Jackson Immuno) coupled with peroxidase with diaminobenzidine as a color substrate and hematoxylin nuclear counterstain, or by fluorescently labeled secondary antibody. Images were acquired on an upright Olympus BX51 microscope equipped with an Olympus DP71 CCD camera, and assembled and labeled in Adobe Photoshop. Confocal series of anti-Cx43 labeling were collected on an Olympus confocal microscope using 40× oil immersion lens, and quantified using ImageJ as described [22]. Briefly, the signal from the red channel (Cx43 signal) was thresholded, and the resulting area of punctate immunopositivity was measured in pixels. Same procedure was performed for the autofluorescence channel, with the resulting tissue area used as 100%. Ratio of Cx43-positive area to total tissue area was then calculated, and expressed as percentage.

3. Results

The activation of the ED10.5 atria originated in an area right from the midline where the SA node is localized [23], and took on average 6 (n = 8) ms (Fig. 3). Same activation pattern, but almost doubled activation time, was observed in the heterozygotes (n = 17). The homozygotes showed a wide range (11–92, n = 13) of activation times, some within the range of the heterozygotes, but some extremely long close to 100 ms.

In ED12.5 mouse embryos, the atrial appendages were small and the atria were clearly visible in frontal view (Fig. 1). We thus analyzed the spreading and the pattern of activation in the antero-superior view, after careful removal of the outflow tract.

The prototypical atrial activation patterns observed in our recordings are shown in Fig. 2. In WT mice (n = 19) the activation pattern was quite uniform among samples. The first epicardial breakthrough (the site of the first electrical activation) was located between the right and left atrium in the roof of the right atrium at the entrance of the superior caval vein, in the place where the sinoatrial node is known to be located at these embryonic stages [24–26]; the signal then spread to both atria, with the right atrium being activated sooner. There was a clear preference for activation spreading along the roof first, resulting in the atrial appendages being activated from the top towards their junction with the ventricles (Fig. 2). The average time of total atrial activation was also evaluated (7 ms; see Fig. 3). Conduction velocity in the right atrium was 15.6 ± 7.0 cm/s; conduction was significantly slower in the left atrium (11.5 ± 3.3 cm/s).

In *Cx40*+/− mice (n = 12) we saw an identical activation pattern. The first breakthrough was in the SAN area, but the average time of atrial activation was significantly prolonged compared to controls; it took on average 9 ms to activate both atria. Conduction velocity was significantly slower than in the wild type in the right atrium (10.8 ± 3.1 cm/s) but not in the left one (10.8 ± 3.3); the gradient between the atria was absent.

In the hearts deficient of Cx40 (*Cx40*−/−) we generally saw two patterns of activation. Only 6 of the 18 hearts analyzed at ED12.5 showed the typical pattern observed in WT hearts (i.e., activation from the SAN area); in the remaining 12 hearts an ectopic focus of the first electrical activation in the right atrial appendage was detected (Fig. 2). Moreover, we found that the total atrial activation times differed depending on the site of activation. In the case of activation from the SAN area, the average time of activation was 19 ms vs. 28 ms necessary for atrial activation from the ectopic site. These differences were statistically significant (Fig. 3). Analysis of atrial activation dynamics showed graphically that the prolongation of total activation time was due to a delay in activation between the right and left atrium, apparent as a change in slope between 40% and 60% of activated atrial area (Fig. 2). Conduction velocities were significantly slower than both wild type and heterozygous animals in both right (5.1 ± 1.9 cm/s) and left (4.4 ± 0.8), which were not, however, significantly different from each other (P = 0.28). The conduction velocity also did not differ between SA-originating and ectopic beat in neither left nor right atrium; thus, the increased total activation time could be attrib-

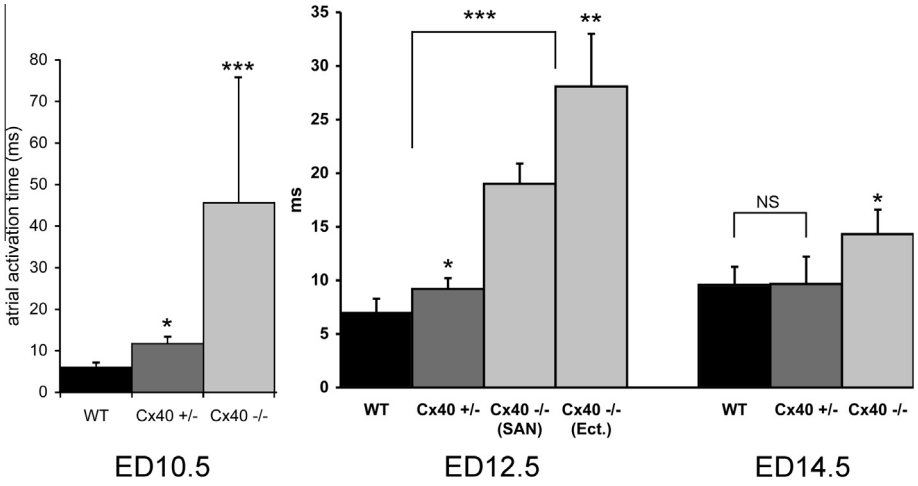

Fig. 3. Activation times of atria at ED10.5 to ED 14.5. The values are means ± S.D. ED10.5: *statistically significant vs. WT; ***statistically significant vs. both WT and heterozygotes. ED12.5: *statistically significant vs. WT; **statistically significant vs. SAN activation; ***either Cx40−/− group is significantly different vs. both WT and Cx40+/− hearts. ED14.5: *significantly different vs. both WT and Cx40+/− hearts. There is no difference between WT and Cx40+/− hearts (NS). Total activation times are based on isochronal maps shown in Fig. 2, with numbers over 10 per group. Compared by ANOVA and Scheffe' test for multiple comparisons.

uted to longer pathway the impulse had to travel from the ectopic site (Fig. 2). The frequency of this ectopic pacemaker was regular and it did not migrate during the individual recordings.

We also tried to analyze the hearts at ED14.5 in the same way, but at this stage the atrial appendages protrude forward, making it difficult to get both them and the back of the atria into the same focal plane without mechanically deforming their shape (such a thing could affect the activation properties of the atria). Nevertheless, we can conclude from our data that the activation patterns remained the same: in WT hearts ($n = 5$) the predominant pattern was still the activation from the SAN area, and in Cx40−/− ($n = 11$) there were the same two patterns of activation described above. The activation times were likewise prolonged in the Cx40 deficient mice (Fig. 3); there was no significant difference between the wild type and the heterozygotes ($n = 9$).

We were also interested in the frequency of spontaneous atrial rhythm. The average rate of the WT atria at ED12.5 *in vitro* was 96 ± 28 bpm. When the activation originated in the SAN, the frequency was similar – in Cx40+/− it was 92 ± 29 bpm, and in Cx40−/− 85 ± 25 bpm (P = NS). There was a big variation in frequencies in the ectopically activated atria – the average frequency was higher at 116 ± 53 bpm, but the difference was not statistically significant.

Having observed all this, we hypothesized that this focus might have a morphological substrate (e.g., some kind of ectopic SA node). Therefore, we examined microscopically serial sections of the hearts of ten Cx40−/− and six WT mice embryos at ED12.5 and ED14.5 stained with an anti-HCN4 antibody detecting an ion channel responsible for autonomic electrical activity in the cells, and found no evidence of HNC4-positive cells in the right appendage in Cx40 mutants (Supplemental Fig. 1). HNC4 expression was detected in the posterior wall of the right atrium as well as around the orifice of the pulmonary vein, which corresponds with the whole mount in situ hybridization study by Garcia-Frigola et al. [23]. Lower levels of HNC4 signal were found throughout the atria and even lower signal, but clearly above background, was present in the ventricles (Supplemental Fig. 1). Staining of neighboring (sister) sections with wheat germ agglutinin did not reveal any significant increase of fibrosis, which was minimal in the atrial tissue (data not shown). Scanning electron microscopy was also performed to complement the morphological evaluation of the atria (data not shown) and revealed no significant changes in atrial morphology or arrangement of the pectinate muscles.

To study possible compensatory changes caused by expression of Cx43, we performed immunohistochemical reaction on adjacent sections from ED10.5, 12.5, and 14.5 hearts. No signal was present at ED10.5, in agreement with previous in situ hybridization study by Delorme and associates [7]. There was an increase in immunoreactivity (+96% WT, +36% Cx40−/−) between ED12.5 (0.46 ± 0.10% WT, 0.29 ± 0.05 Cx40−/−) and 14.5 (0.90 ± 20.6% WT, 0.39 ± 0.15 Cx40−/−). with increased localization of the particles to the cell membrane (Supplemental Fig. 2). There was a trend towards lower Cx43 levels in the Cx40−/− atria (−37%, $P = 0.047$ at ED12.5 and −57%, $P = 0.097$ at ED14.5).

4. Discussion

The role of Cx40 in cardiac arrhythmogenesis has been described earlier by a number of research groups [9,10,13]. Despite this, the functional role of this protein in development is still not fully understood. Our study contributes to this understanding with the following conclusions: (1) The lack of Cx40 in the embryonic atria directly influences the conduction properties of atrial myocardium (see Fig. 3). This is consistent with the fact that Cx40 is the main gap junction protein in murine atria [6]. The function of missing Cx40 could be substituted by other connexins, especially Cx43. According to the study by Delorme et al., the expression of *Cx43* in mouse atria is detectable by *in situ hybridization* from ED12.5 onwards [7]. In our data, the prolongation of activation times in Cx40 deficient atria compared to WT is much higher at ED10.5 or 12.5 (more than 3 times longer) in contrast to ED14.5 (only about 30% more, see Fig. 3), suggesting a mechanism of developmental compensation from the 43 isoform. Lower levels of Cx43 observed in Cx40−/− are not likely biologically significant, as the amounts must be decreased by more than 90% to observe physiological phenotype. (2) In 2/3 of *Cx40*−/− embryonic hearts at ED12.5, the first breakthrough was located in an ectopic site in the right atrium without the presence of any morphological or molecular substrate that could explain these autorhythmic properties; this might reflect an abnormal exit [27] of the impulse from the SAN. However, study performed in the adult Cx40−/− mice indicated that there are truly ectopic foci, since their ablation resulted in re-location of the pacemaker back to the SA node, although with much reduced frequency [16]. Accordingly, we did not find any morphological changes in SA node formation in

Cx40 deficient hearts (Supplemental Fig. 1). The frequency of atrial pacing from ectopic foci was rather irregular, suggesting also a functional problem. (3) When the excitation was spreading from this ectopic place, the activation time of both atria was even more prolonged than in the rest of the CX40−/−. We hypothesize that this could be a consequence of the presence of a preferential pathway (Bachmann's bundle) of signal spreading from the SAN to the left atrium, as described in the chick embryos [28] as well as other species [29] including humans [30]. This preferential pathway does not seem to be fully utilized during the ectopic activation (Fig. 2), resulting in prolonged conduction through the working right atrial myocardium with the interatrial septum causing a further delay by acting like a sink. However, the conduction velocity did not differ significantly between the SA-originating and ectopic activation in neither left nor right atrium of the CX40−/− deficient hearts; thus, the increased activation time could be attributed to the prolonged pathway the impulse had to travel from the ectopic site.

Verheule et al. described several cardiac conduction abnormalities in adult mice lacking Cx40 [12]. They found a P wave prolongation on surface electrocardiographs (corresponding to the atrial activation time) and a 30% decrease in the conduction velocity in *Cx40*−/− mice compared with the WT. In addition, burst pacing was able to provoke atrial tachyarrhythmias in 50% of the mutants. This prolongation of atrial activation time is quantitatively very similar to our results at ED14.5, and such slowing of conduction velocity could be one of the arrhythmogenic factors in human cases of Cx40 disruption.

This is the first study that maps in detail the effect of CX40 deficiency on activation spreading and times of murine embryonic atria at and before ED12.5. Leaf et al. performed an extensive study about the effect of Cx40 on conduction heterogeneity in adult mice of a wide range of ages as well as in embryos (ED13.5 and ED15.5) [17]. These authors also showed the amount of Cx40 protein is reduced by approximately 50% in the *Cx40*+/− atria. In their study they detected the presence of more ectopic sites of activation at ED15.5, localized also in the left atrium, whereas at ED13.5 they described normal SA node activation both in *Cx40*+/+ and in *Cx40*−/− mice. This is in contrast with our data, as we found ectopic activation already at ED12.5 in two thirds of the hearts. Such a discrepancy can be due to a different method of gene deletion (unlike Leaf et. al. we used GFP:Cx40 knock-in mouse line), and/or to the influence of different genetic background of the strains, and/or to slightly different methodological approaches (we did not use signal averaging and motion tracking in our optical recordings). Interestingly, we were unable to correlate the ectopic pacemaker with any morphological substrate, either fibrosis with myofibrillar disarray, or abnormal pacemaking channel expression domain.

In conclusion, this study shows that a lack of Cx40 in atria during development influences the activation patterns of spontaneous impulse propagation and significantly slows impulse propagation velocity (which directly correlates with the type of atrial activation). The most significant effect is observed at the earliest stages, where the expression of Cx43 does not compensate for the deficiency of Cx40. This study improves our understanding about the electrophysiological function of Cx40 during embryonic development and the relationship between the activation times of atria, the amount of Cx40 and the site of activation.

Conflict of interests

Neither author reports any conflict of interests.

Acknowledgements

Our sincere thanks are due to Dr. Lucile Miquerol, IBDM, France, for supplying the *Cx40*−/− mice. We would like to thank Ms. Marie Jindrakova, Marketa Pleschnerova, Jarmila Svatunkova and Eva Kluzakova for their excellent technical assistance. Mr. Frantisek Alferi performed acquisition and quantification of the Cx43 and HCN4 immunostaining. Supported by the Ministry of Education PRVOUK-P35/LF1/5, and institutional RVO: 67985823. Further support comes from the Grant Agency of the Czech Republic 13-12412S, P302/11/1308, and 204/09/H084. J.B. and B.S. are supported by a training fellowship program of Charles University in Prague, First Faculty of Medicine.

Appendix A. Supplementary data

Supplementary data associated with this article can be found, in the online version, at http://dx.doi.org/10.1016/j.febslet.2014.01.032.

References

[1] van der Velden, H.M., van Kempen, M.J., Wijffels, M.C., van Zijverden, M., Groenewegen, W.A., Allessie, M.A. and Jongsma, H.J. (1998) J. Cardiovasc. Electrophysiol. 9, 596–607.
[2] Kirchhoff, S., Nelles, E., Hagendorff, A., Kruger, O., Traub, O. and Willecke, K. (1998) Curr. Biol. 8, 299–302.
[3] Simon, A.M., Goodenough, D.A. and Paul, D.L. (1998) Curr. Biol. 8, 295–298.
[4] Kanter, H.L., Saffitz, J.E. and Beyer, E.C. (1992) Circ. Res. 70, 438–444.
[5] Gros, D.B. and Jongsma, H.J. (1996) Bioessays 18, 719–730.
[6] Jalife, J., Morley, G.E. and Vaidya, D. (1999) J. Cardiovasc. Electrophysiol. 10, 1649–1663.
[7] Delorme, B., Dahl, E., Jarry-Guichard, T., Briand, J.P., Willecke, K., Gros, D. and Theveniau-Ruissy, M. (1997) Circ. Res. 81, 423–437.
[8] Moorman, A.F. and Christoffels, V.M. (2003) Physiol. Rev. 83, 1223–1267.
[9] Dupont, E. et al. (2001) J. Mol. Cell. Cardiol. 33, 359–371.
[10] Polontchouk, L. et al. (2001) J. Am. Coll. Cardiol. 38, 883–891.
[11] Kanagaratnam, P. and Peters, N.S. (2004) Heart Rhythm 1, 746–749.
[12] Verheule, S., van Batenburg, C.A., Coenjaerts, F.E., Kirchhoff, S., Willecke, K. and Jongsma, H.J. (1999) J. Cardiovasc. Electrophysiol. 10, 1380–1389.
[13] Hauer, R.N., Groenewegen, W.A., Firouzi, M., Ramanna, H. and Jongsma, H.J. (2006) Adv. Cardiol. 42, 284–291.
[14] Yang, Y.Q., Zhang, X.L., Wang, X.H., Tan, H.W., Shi, H.F., Jiang, W.F., Fang, W.Y. and Liu, X. (2010) Int. J. Mol. Med. 26, 605–610.
[15] Tamaddon, H.S., Vaidya, D., Simon, A.M., Paul, D.L., Jalife, J. and Morley, G.E. (2000) Circ. Res. 87, 929–936.
[16] Bagwe, S., Berenfeld, O., Vaidya, D., Morley, G.E. and Jalife, J. (2005) Circulation 112, 2245–2253.
[17] Leaf, D.E. et al. (2008) Circ. Res. 103, 1001–1008.
[18] Miquerol, L. et al. (2004) Cardiovasc. Res. 63, 77–86.
[19] Sankova, B., Benes, J., Jr., Krejci, E., Dupays, L., Theveniau-Ruissy, M., Miquerol, L. and Sedmera, D. (2012) Cardiovasc. Res. 95, 469–479.
[20] Sankova, B., Machalek, J. and Sedmera, D. (2010) Am. J. Physiol. Heart Circ. Physiol. 298, H1571–H1576.
[21] O'Quinn, M.P., Palatinus, J.A., Harris, B.S., Hewett, K.W. and Gourdie, R.G. (2011) Circ. Res. 108, 704–715.
[22] Benes Jr., J., Melenovsky, V., Skaroupkova, P., Pospisilova, J., Petrak, J., Cervenka, L. and Sedmera, D. (2011) Anat. Rec. (Hoboken) 294, 102–111.
[23] Garcia-Frigola, C., Shi, Y. and Evans, S.M. (2003) Gene Expr. Patterns 3, 777–783.
[24] Liu, J., Dobrzynski, H., Yanni, J., Boyett, M.R. and Lei, M. (2007) Cardiovasc. Res. 73, 729–738.
[25] Mommersteeg, M.T. et al. (2007) Circ. Res. 100, 354–362.
[26] Viswanathan, S., Burch, J.B., Fishman, G.I., Moskowitz, I.P. and Benson, D.W. (2007) J. Mol. Cell. Cardiol. 42, 946–953.
[27] Verheijck, E.E., van Kempen, M.J., Veereschild, M., Lurvink, J., Jongsma, H.J. and Bouman, L.N. (2001) Cardiovasc. Res. 52, 40–50.
[28] Sedmera, D., Wessels, A., Trusk, T.C., Thompson, R.P., Hewett, K.W. and Gourdie, R.G. (2006) Am. J. Physiol. Heart Circ. Physiol. 291, H1646–H1652.
[29] Dolber, P.C. and Spach, M.S. (1989) Am. J. Physiol. 257, H1446–H1457.
[30] Ho, S.Y., Anderson, R.H. and Sanchez-Quintana, D. (2002) Cardiovasc. Res. 54, 325–336.